

# Understanding the mobility of nonspherical particles in the free molecular regime

Mingdong Li, George W. Mulholland, and Michael R. Zachariah\*

*Department of Chemical and Biomolecular Engineering, University of Maryland, College Park, Maryland, USA*

*Department of Chemistry and Biochemistry, University of Maryland, College Park, Maryland, USA*

*and National Institute of Standards and Technology, Gaithersburg, Maryland, USA*

(Received 18 October 2013; published 10 February 2014; corrected 12 February 2014)

An approach to obtain the mobility of nonspherical particles is proposed by averaging the drag force orientationally, and two other widely used approaches in the literature, the averaged-collision-integral and averaged-drift-velocity methods, are summarized and extended. The concept of orientationally averaged collision integrals based on Chapman-Enskog theory for small gas-phase ions is re-examined for macromolecular ions whose surface cannot be treated as specular, but with inelastic interactions. A well accepted collision model considering inelastic collisions is Epstein's theory, which has been extended to include long-range potential forces by Li and Wang [*Phys. Rev. E* **68**, 061206 (2003)] for spherical particles. This work extends Li and Wang's spherical particle theory to convex nonspherical particles considering long-range potential, and simplifies this collision integral to a product of the averaged projection area and an enhancement factor for short-range interactions (hard collisions), which is independent of convex particle shape and is identical to the value for a sphere that people are using. We also show that the averaged projection area of a convex particle in free molecular regime for hard collisions is equal to its mobility diameter. The second approach is the averaged-drift-velocity approach using the friction coefficient in a tensor form, which is often employed in aerosol science. We extend this approach in our previous work for axisymmetric particles to develop an expression for the mobility of nonspherical particles in a general form. Furthermore, it is pointed out that this approach is only valid when the particle Brownian rotation is slow compared with the particle translational relaxation time. If the particle Brownian rotation is fast, usually so in the case of very small ions and particles, we propose an "averaged-drag-force" approach. The three approaches are then compared for a randomly oriented rod and the protein GroEL. We show that for a cylinder rod in the free molecular regime at random orientation, the averaged-drag-force approach is identical to the averaged-collision-integral approach for short-range interactions (hard collisions). We then summarize the relationship between collision-integral based approach and tensor based approaches. For readers only interested in implementation of the theory, we provide useful expressions in Tables I and II.

DOI: [10.1103/PhysRevE.89.022112](https://doi.org/10.1103/PhysRevE.89.022112)

PACS number(s): 05.20.Dd, 47.45.Dt, 05.60.Cd, 81.20.Rg

## I. INTRODUCTION

Mobility as an important particle transport property is critical to the measurement of the dynamics of gas-phase ions and nanoparticles in fluids, and of interest to a wide range of research including the structure study of atomic clusters, macromolecules [1–4], and in aerosol science [5–8]. The relationships between mobility and diameter of a specular spherical ion in a gas and a spherical particle in a gas are well established and governed by Chapman-Enskog theory [8] (Ferziger and Kaper, 1972, Sec. 7.3) [9] and the Stokes-Cunningham formula [8,10], respectively. However, most ions and particles are nonspherical and the relationship between geometric shape and mobility is much more complicated.

Mason and McDaniel [11] extended the Chapman-Enskog theory for the mobility of a nonspherical small ion by calculating its orientationally averaged collision integral. This has been widely applied to structure determination of molecular clusters [12] and macromolecules, including proteins and their complexes [4,13] using ion mobility spectrometry (IMS) combined with mass spectrometry (MS). There are two basic approaches to determine the orientationally averaged collision integral: projected area (PA) [1] and exact hard-spheres scattering (EHSS) [2]. The structure of a molecular cluster

or a macromolecule can then be determined by comparing the measured mobility, with the calculated mobility based on either of the two collision integrals for an assumed molecular structure. However, when an ion becomes large, and approaches the size of an aerosol particle (a few nanometers [7]), the surface of the particle relative to very small gas molecules cannot be treated as a simple specular surface, but rather a surface with inelastic interactions (or energy interconversion between the kinetic energy of a gas molecule and the internal energy of the target particle) [14,15], thus the above relationships between mobility and the two collision integrals used for small ions need to be reexamined. The PA projected area method has been extended to a projected superposition approximation (PSA) method to account for a shape factor and to adjust the atom size as a function of temperature [16,17]. However, the PSA method is still an elastic model, and the shape factor using this PSA method only considers the roughness of the particle surface. For a spherical particle in the free molecular regime, Epstein [14] proposed an accommodation factor  $f$  to incorporate inelastic collisions (or diffuse reflections) for spheres with short-range interactions (hard collisions), resulting in an enhancement factor  $\xi = 1 + \pi f/8$  compared with the drag force for small molecules with fully specular reflections from Chapman-Enskog theory. Tammet [15] suggested this enhancement factor is 1.32 for macroscopic spherical particles, and Hogan and de la Mora [18] used a value 1.36 based on spherical

\*mrz@umd.edu

symmetry. In the literature, this enhancement factor derived from spheres has been widely applied to nonspheres without rigorous consideration [16,19].

Recently, Larriba and Hogan developed a calculational approach to consider diffusion scattering for collision integral calculations [20,21]. In this work, we propose a simpler expression for the orientationally averaged collision integral for nonspherical particles based on extending the approach of Li and Wang [8] used for spherical particles. For short-range interactions (hard collisions) we show that the collision integral for a convex particle simplifies to the product of the averaged projection area multiplied by the  $1 + \pi f/8$  factor. Furthermore, by connecting the extended Epstein expression to the Stokes-Cunningham expression for a nonspherical convex particle for short-range interactions (hard collisions), the averaged projection area diameter for a convex particle in the free molecular regime is shown equal to the mobility diameter.

Another approach to obtain the mobility of nonspherical particles is the averaged-drift-velocity approach proposed by Happel and Brenner [22] for particles in low Reynolds number flows. Beginning with the friction coefficient expressed in a tensor form, the averaged mobility or averaged drag force of a randomly oriented particle is obtained by averaging the drift velocity of the particle by equating the drag force to the external force for each particle orientation. This quasiequilibrium approach has been widely used in the study of aerosol particles in all three regimes: free molecular, transition, and continuum regimes [23–27]. Dahneke [24] employed this approach to obtain the randomly oriented resistance coefficient of straight-chain aggregates of uniform spheres in all three regimes. Mackowski [27] employed this approach for simulating the averaged drag force acting on a randomly oriented cluster in the free molecular regime. We (Li *et al.*) [28] extended this approach for axisymmetric particles allowing for a Boltzmann orientation distribution arising from the competition between Brownian motion and the alignment of nonspherical particles in an electric field, which has been experimentally verified using a monodisperse gold nanorod [5,29].

In this work, we extend this approach (averaged-drift-velocity) further to a convex particle with any shape. However, this approach (averaged-drift-velocity) implicitly assumes that the particle Brownian rotation is slow compared with the particle translational relaxation time [30], so that at each orientation the drag force is immediately balanced by the external force. On the other hand if particle Brownian rotation is fast compared with the particle translational relaxation time, i.e., typically for small ions and for particles in the free molecular regime, we develop an averaged-drag-force approach using the friction coefficient in tensor form. The mobility diameters from the averaged-drift-velocity approach and from the averaged-drag-force approach can be treated as two theoretical limit diameters.

The mobility diameters for the same particle computed by the three approaches (averaged-collision integral, averaged-drift velocity, and averaged-drag force) are then compared with each other for randomly oriented rods. For a cylinder rod in the free molecular regime at random orientation, the averaged-drag-force approach is shown to be identical to the averaged-collision-integral approach for a short-range interaction (hard collision). We also compare the calculation results of the three approaches to experimental values of gold nanorods, which is a rigid rod with dimensions (from TEM) 17 nm  $\times$  270 nm, and show that the experimental mobility diameter falls between the two limit diameters from the averaged-drift-velocity and from the averaged-drag-force approach. Finally, the calculation results of the three approaches are compared with the calculation results for the protein GroEL.

For readers only interested in implementation of the theory, we provide the working formulas in Table I and II.

## II. THEORY

We begin with a summary of the relevant expressions that result from the three approaches to be developed and discussed in this paper. Some readers may wish to skip some of the detailed derivations and proceed directly to Sec. III. The three approaches in this section for the expressions of drag force and electric mobility are presented in Table I.

TABLE I. Summary of resulting working expressions from the three approaches (in Sec. II) for the drag force and electric mobility of nonspherical particles.<sup>a</sup> The criterion for a rod was described in Li (2012, pp. 165–169) [30] to assess if Brownian motion of a cylindrical particle is slow or fast by scaling to the particle translational relaxation time to determine which approach applies. In Li (2012, pp. 165–169) [30], a characteristic time  $\tau_0$  was defined for Brownian rotation, and compared with the translational relaxation time  $\tau_{t,rod} = m/K_{random}$ , where  $m$  is the mass of the rod,  $1/K_{random} = 2/K_1 + 1/K_3$ , and  $K_1, K_3$  were given in Sec. IVA for a rod in the free molecular regime. If  $\tau_0/\tau_{t,rod} < 1$ , then Brownian rotation is considered fast, and the averaged-drag-force approach applies; if  $\tau_0/\tau_{t,rod} > 482$ , Brownian rotation is considered slow, and the averaged-drift-velocity approach applies; and if  $\tau_0/\tau_{t,rod}$  falls in between, it is a mixed picture.

Approach	Criterion for a rod	Drag force and mobility	Eq.
Approach I: Avg $\langle \Omega \rangle$	$\tau_0/\tau_{t,rod} < 1$	$\vec{F}_{drag} = -\frac{8}{3}\sqrt{\frac{2m_r k_B T}{\pi}} N \langle \Omega \rangle \vec{V}_d,$	(1)
		$Z_p = \frac{3q}{16N} \sqrt{\frac{2\pi}{m_r k_B T}} \frac{1}{\langle \Omega \rangle},$	(3)
		where $\langle \Omega \rangle$ is given by Eq. (5)	
Approach II: Avg $\langle \vec{V}_d \rangle$	$\tau_0/\tau_{t,rod} > 482$	$\vec{F}_{drag} = -\hat{K} \cdot \vec{V}_d,$	(19)
		$\langle Z_p \rangle_k = q(K_1^{-1} \langle \sin^2 \theta \sin^2 \psi \rangle + K_2^{-1} \langle \sin^2 \theta \cos^2 \psi \rangle + K_3^{-1} \langle \cos^2 \theta \rangle),$	(22)
Approach III: Avg $\langle \vec{F}_{drag} \rangle$	$\tau_0/\tau_{t,rod} < 1$	$\vec{F}_{drag} = -\hat{K} \cdot \vec{V}_d,$	(19)
		$Z_p = q/(K_1 \langle \sin^2 \theta \sin^2 \psi \rangle + K_2 \langle \sin^2 \theta \cos^2 \psi \rangle + K_3 \langle \cos^2 \theta \rangle)$	(27)

<sup>a</sup>The definitions of the symbols in this table refer to Eqs. (1), (3), (5), (19), (22), and (27).

TABLE II. Summary of the working expressions for mobility diameter of nonspherical particles with convex shape undergoing hard collisions (with fully random orientation) using the three approaches (Sec. IV).<sup>a</sup> The criterion for a rod is explained in the caption of Table I.

Approach	Criterion for a rod	Mobility diameter	Eq.
Approach I: Avg $\langle \Omega \rangle$ for hard collisions	$\tau_0/\tau_{t,\text{rod}} < 1$	$d_m = d_{\text{pa}}$	(18)
Approach II: Avg $\langle \vec{V}_d \rangle$	$\tau_0/\tau_{t,\text{rod}} > 482$	$\frac{2\lambda(A_1+A_2)q}{3\pi\eta d_m^2} = \frac{1}{3}q\left(\frac{1}{K_1} + \frac{1}{K_2} + \frac{1}{K_3}\right)$	(23), (30)
Approach III: Avg $\langle \vec{F}_{\text{drag}} \rangle$	$\tau_0/\tau_{t,\text{rod}} < 1$	$\frac{2\lambda(A_1+A_2)q}{3\pi\eta d_m^2} = \frac{3q}{K_1+K_2+K_3}$	(28), (30)

<sup>a</sup>The definitions of the symbols in this table refer to Eqs. (18), (23), (28), and (30).

### A. Approach I: Mobility of a nonspherical particle from the averaged-collision-integral

The momentum transfer (or drag force) between a small spherical ion and gas molecules is determined by the collision integral  $\Omega^{(1,1)}$  (or simply  $\Omega$ ) and governed by the Chapman-Enskog relationship [8,9]. Mason and McDaniel [11] extended it to a nonspherical small ion by replacing  $\Omega$  with an orientationally averaged collision integral  $\langle \Omega \rangle$ ,

$$\vec{F}_{\text{drag}} = -\frac{8}{3}\sqrt{\frac{2m_r k_B T}{\pi}} N \langle \Omega \rangle \vec{V}_d, \quad (1)$$

$$\langle \Omega \rangle = \frac{1}{8\pi^2} \int_0^{2\pi} d\varphi \int_0^\pi d\theta \sin\theta \int_0^{2\pi} d\psi \Omega(\varphi, \psi, \theta), \quad (2)$$

where  $N$  is the gas number density,  $m_r$  is the reduced mass,  $k_B$  is the Boltzmann constant,  $T$  is the gas temperature,  $V_d$  is the ion drift velocity, and  $\varphi, \psi, \theta$ , are the Euler angles to determine orientations of ions (see Appendix A, Fig. 1). By equating the averaged drag force  $\langle F_{\text{drag}} \rangle$  to the external force  $F_{\text{ext}} = qE$  in an electric field  $E$ , where  $q$  is the free charge on the small ion, the electric mobility of small nonspherical ion (or particle) is obtained:

$$Z_p = \frac{V_d}{E} = \frac{3q}{16N} \sqrt{\frac{2\pi}{m_r k_B T}} \frac{1}{\langle \Omega \rangle}. \quad (3)$$

There are three implicit assumptions in the derivations above. First, the collision between an ion and gas molecules are elastic. Second, the drift velocity is assumed independent of ion orientation, which is valid for small ions and for small particles undergoing rapid rotation, and will be discussed in Sec. IV. The third assumption is that the expression of the collision integral of a nonspherical ion or particle at a given orientation, that is, with fixed  $(\varphi, \psi, \theta)$ , has similar form as for a sphere with the corresponding scattering angle. Thus the use of Eq. (3) for nonspheres is reasonable by averaging the scattering-collision integral over all orientations. This method has been heavily employed in the study of macromolecular ions such as proteins and other biological particles. Typically, the expressions of collision integral  $\Omega$  (projection, trajectory, and projected superposition) are only based on elastic collisions [2,3,16,31]. However, when an ion becomes large and approaches the size of an aerosol particle, the surface of the particle relative to small gas molecules cannot be treated as a simple elastic surface. Rather one should consider a surface with inelastic interactions between a gas molecule and the internal energy of the relatively large particle [14,15].

For a spherical particle with hard collisions, Epstein [14] incorporated inelastic collisions by using an accommodation factor, which was extended by Li and Wang [8] to include long-range potential forces for a spherical particle,

$$\Omega = \Omega_{\text{Epstein}} = f\Omega_d + (1-f)\Omega_s, \quad (4)$$

where  $\Omega_s$  is the specular-scattering collision integral,  $\Omega_d$  is the diffuse-scattering collision integral [8], and  $f$  is a switching function (or momentum accommodation factor). Epstein's approach assumes that a fraction of gas molecules,  $f$ , that collides with the particle surface are instantaneously absorbed on the surface and then re-emitted with a Maxwell velocity distribution corresponding to the temperature of the surface. Thus,  $f$  represents the fraction of diffuse reflections. Ku and de la Mora reported  $f \sim 0.9$  for larger than 1.3 nm nanodrops [7]. In both scattering situations, the particle surface is treated as a smooth surface.

For nonspheres we propose an orientationally averaged collision integral approach to obtain the drag force and mobility of a convex nonspherical particle in the free molecular regime by extending Li and Wang's theory [8] to obtain

$$\langle \Omega \rangle = \langle \Omega_{\text{Epstein}} \rangle = f\langle \Omega_d \rangle + (1-f)\langle \Omega_s \rangle, \quad (5)$$

where  $\Omega_s$  and  $\Omega_d$  are derived in Appendix C, Eqs. (C2) and (C3); for the case of short-range interactions (hard collisions),  $\Omega_s$  and  $\Omega_d$  are equivalent to cross sections  $Q_s$  and  $Q_d$ , where  $Q_s$  is given by [8,32]

$$\Omega_s = Q_s = 2\pi \int_0^{b_{\text{max}}} b[1 - \cos\chi]db \quad (6)$$

and  $Q_d$  is derived in the Appendix C as

$$\Omega_d = Q_d = 2\pi \int_0^{b_{\text{max}}} b \left[ 1 + \frac{3\pi}{16} \sin\frac{\chi}{2} \right] db, \quad (7)$$

where  $b$  is the impact parameter, and  $\chi$  is the scattering angle. With the orientationally averaged collision integral  $\langle \Omega \rangle$  for a nonspherical convex particle in Eq. (5), the drag force and the mobility are given by Eqs. (1) and (3) respectively.

The orientationally averaging defined in Eq. (2) is assuming random orientations. To consider orientations following a distribution probability function  $f(\varphi, \psi, \theta)$ , the averaged collision integral could be defined as

$$\langle \Omega \rangle = \int_0^{2\pi} d\varphi \int_0^\pi d\theta \sin\theta \int_0^{2\pi} d\psi f(\varphi, \psi, \theta) \Omega(\varphi, \psi, \theta), \quad (8)$$

where

$$\int_0^{2\pi} d\varphi \int_0^\pi d\theta \sin\theta \int_0^{2\pi} d\psi f(\varphi, \psi, \theta) = 1. \quad (9)$$

The orientational probability function  $f(\varphi, \psi, \theta)$  due to Brownian rotation is discussed in Appendix B.

We note here that in the extended Epstein's approach, that is, Eq. (5), both  $\langle\Omega_s\rangle$  and  $\langle\Omega_d\rangle$  should be calculated assuming the particle surface is smooth. For spheres (radius  $R$ ) undergoing hard collisions, the integrals in Eqs. (6) and (7) can be evaluated analytically with the result  $\Omega_s = \pi R^2$  and  $\Omega_d = (1 + \pi/8)\pi R^2$ . Shvartsburg and Jarrold [2] showed that for nonspherical particles with convex shape undergoing hard specular collisions the total averaged cross integral is the sum of the averaged cross integrals of infinitesimally small surfaces. Extending this result, we show in Appendix C that the averaged collision integral  $\langle\Omega\rangle$  in Eq. (5) for nonspherical particles with convex shape undergoing hard collisions (including both specular and diffusion collisions) can be simplified to the averaged projected area multiplied by a factor

$$\langle\Omega\rangle = \left(1 + \frac{\pi f}{8}\right) \langle Q_{\text{pa}}\rangle = \xi \langle Q_{\text{pa}}\rangle, \quad (10)$$

where

$$\xi = 1 + \frac{\pi f}{8} \quad (11)$$

is ‘‘the enhancement factor’’ used in literature.  $\langle Q_{\text{pa}}\rangle$  is the averaged projection area over all orientations of particle (or ion) [averaging refers to Eq. (2)], and  $Q_{\text{pa}}(\varphi, \psi, \theta) = \int_{-\infty}^{+\infty} \int_{-\infty}^{+\infty} M(\varphi, \psi, \theta, x, y) dx dy$  is the projected area (or shade area) at a particular orientation  $(\varphi, \psi, \theta, \dots)$  (Appendix A, Fig. 1) in a Cartesian coordinates inside a rectangle with sides along the  $x$  and  $y$  axes, and  $M$  is unity when a hard collision occurs and zero otherwise [1,3]. The averaged projection area of particles with any shape can be calculated using the open source software program MOBCAL [2,4].

It is noteworthy that the orientationally averaged collision integral for a convex nonspherical particle calculated in Eq. (5) is simplified to the averaged projection area with a factor for hard collisions, which is independent of the shape of a convex particle and is identical to the value for a sphere in the literature. For a small specular convex ion with hard collisions, the averaged collision integral  $\langle\Omega\rangle$  is equal to the averaged projection area  $\langle Q_{\text{pa}}\rangle$ , while for a convex particle including diffuse collisions, there is an enhanced factor  $1 + \pi f/8$ . Tammet [15] assigns the enhancement factor a value of 1.32 for macroscopic spherical particles, and Hogan *et al.* [18,19] used 1.36 for small and large protein particles, both based on Epstein's spherical theory. In this work above, we derived the same expression for a convex nonspherical ion or particle, and showed it as the ratio between the true collision integral and the projected area for hard collisions. For a small specular ion, this factor,  $1 + \pi f/8$ , is unity with  $f \sim 0$  based on Chapman-Enskog theory [8] (Ferziger and Kaper, 1972, Sec. 7.3) [9], while for a relatively big ion or particle (Ku and de la Mora reported  $f \sim 0.9$  for larger than 1.3-nm nanodrops [7]), this enhanced factor is greater than 1. We note that this expression of enhanced factor in Eqs. (10) and (11) is only valid for short-range interactions (hard collisions). For the general expressions for averaged collision integral  $\langle\Omega\rangle$  and for the enhanced factor which is defined as the ratio between  $\langle\Omega\rangle$  and  $\langle Q_{\text{pa}}\rangle$ , one should use Eq. (5) and the collision integrals,

$\langle Q_s\rangle$  and  $\langle Q_d\rangle$ , derived based on Li and Wang [8] given in Appendix C, Eqs. (C2) and (C3).

For short-range interactions, combining Eqs. (1) and (10), we obtain the drag for a convex hard-body particle,

$$\vec{F}_{\text{drag}} = -\frac{8}{3}\xi\sqrt{\frac{2m_r k_B T}{\pi}} N \langle Q_{\text{pa}}\rangle \vec{V}_d. \quad (12)$$

Or, the mobility is

$$Z_p = \frac{1}{\xi} \frac{3q}{16N} \sqrt{\frac{2\pi}{m_r k_B T}} \frac{1}{\langle Q_{\text{pa}}\rangle}. \quad (13)$$

If we define an averaged projection area diameter as  $d_{\text{pa}} = \sqrt{4\langle Q_{\text{pa}}\rangle/\pi}$ , then Eq. (12) becomes

$$\vec{F}_{\text{drag}} = -\frac{2}{3}\xi\sqrt{2\pi m_r k_B T} N d_{\text{pa}}^2 \vec{V}_d \quad (14)$$

which is similar to Epstein's equation for a spherical particle except the diameter of a sphere is replaced by the averaged projection area diameter of a nonspherical convex particle.

**Connecting Epstein to Stokes-Cunningham for a nonspherical convex particle for short-range interactions (hard collisions).** If we consider the expression of coefficient of viscosity in Allen and Raabe (1982) [33],

$$\eta = \phi(Nm_r) \left(\frac{8k_B T}{\pi m_r}\right)^{1/2} \lambda, \quad (15)$$

where  $\phi$  is a constant value, and assume the accommodation factor  $f$  for a nonsphere has the same relationship with Cunningham parameters as for a sphere in free molecular regime as in Allen and Raabe [33,34],

$$f = \frac{1}{\pi} \left(\frac{36\phi}{A_1 + A_2} - 8\right), \quad (16)$$

then Eq. (14) becomes

$$F_{\text{drag}} = -\frac{3\pi\eta d_{\text{pa}}^2 V_d}{2\lambda(A_1 + A_2)}, \quad (17)$$

where  $A_1 = 1.165$  and  $A_2 = 0.483$  for solid particles with averaged free path  $\lambda = 67.3$  nm for ambient air at sea level and 23 °C given by Kim *et al.* [35], which gives  $f = 0.868$  and the enhanced factor  $\xi = 1 + \pi f/8 = 1.34$ . Equation (17) is similar to the Stokes-Cunningham formula for a sphere particle in the free molecular regime except that the diameter of a sphere is replaced by an averaged projection area diameter for a nonspherical convex particle. Since Eq. (17) is exactly the definition of mobility diameter for a nonspherical particle  $d_m$  in the free molecular regime,  $F_{\text{drag}} = -3\pi\eta d_m^2 V_d/2\lambda(A_1 + A_2)$ , it results in

$$d_m = d_{\text{pa}}, \quad (18)$$

that is, the mobility diameter is equal to the averaged projection area diameter for a convex particle for short-range interactions (hard collisions), which is a bridge between the projection calculated diameter and the experimental measured mobility diameter for short-range potentials. We note here that this diameter of a nonspherical particle is averaged over all directions in three dimensions, not just in two dimensions or along three orthogonal directions as is assumed in some examples in the literature [36].

### B. Approach II: Mobility of a nonspherical particle from averaged-drift velocity

The averaged-drift-velocity approach is well accepted for nonspherical particles at low Reynolds number [22]. The reader should keep in mind that this approach is only valid for particles whose Brownian rotation is slow compared to the translational relaxation time [30].

Employing the friction coefficient  $\hat{K}$  in tensor form, the drag force is expressed as [22,28]

$$\vec{F}_{\text{drag}} = -\hat{K} \cdot \vec{V}_d, \quad (19)$$

where  $\vec{V}_d$  is the drift velocity of the particle. The explicit expressions of the three principle components ( $K_1, K_2, K_3$ ) of the friction coefficient tensor for hard-body rods and prolate spheroids were provided in Li *et al.* [28]. A general expression of the friction coefficient tensor  $\hat{K}$  of a convex hard-body particle in the free molecular regime was proposed by de la Mora based on Garcia-Ybarra and Rosner's approach [37,38].

Assuming that at each orientation of the particle the drag force is balanced by the electric force, we obtain

$$\hat{K} \cdot \vec{V}_d = q\vec{E}, \quad (20)$$

and

$$\vec{V}_d = q\hat{K}^{-1} \cdot \vec{E}. \quad (21)$$

The orientation averaged velocity  $\langle \vec{V}_d \rangle$  can be expressed in terms of the Euler angles  $\varphi, \psi, \theta$ , which relate the body fixed coordinate system  $(\vec{i}', \vec{j}', \vec{k}')$  to the space fixed coordinates  $(\vec{i}, \vec{j}, \vec{k})$  (Appendix A), and the orientational probability function  $f(\varphi, \psi, \theta)$ .  $\vec{k}$  is defined as the external force direction, here the electric force. The orientational probability function  $f(\varphi, \psi, \theta)$  due to Brownian rotation is discussed in Appendix B.

In general, the drift velocity  $\vec{V}_d$  of a nonspherical particle in Eq. (21) is orientation dependent, and the orientation averaged velocity  $\langle \vec{V}_d \rangle$  may have components other than in the  $\vec{k}$  direction (external force direction). In such a situation, we can consider the component of the average velocity along the external force direction to define its mobility as

$$\langle Z_p \rangle_{\vec{k}} = \langle V_{d,z} \rangle / E = q(K_1^{-1} \langle \sin^2 \theta \sin^2 \psi \rangle + K_2^{-1} \langle \sin^2 \theta \cos^2 \psi \rangle + K_3^{-1} \langle \cos^2 \theta \rangle). \quad (22)$$

All the averaging above in Eq. (22) is defined in the form of Eq. (8). The derivation of Eq. (22) is shown in Appendix A1.

In some specific situations, the averaged drift velocity  $\langle \vec{V}_d \rangle$  only has one component which is along the external force direction ( $\vec{k}$  direction), that is  $\langle \vec{V}_d \rangle = \langle V_d \rangle \vec{k}$ , and the averaged mobility can be conveniently obtained by  $\langle Z_p \rangle = \langle V_d \rangle / E$ . We discuss three such cases: fully random, axisymmetric particles with orientation distribution  $f(\theta)$ , and a more general symmetric case with orientation distribution  $f(\psi, \theta)$ . The last two cases are shown in detail in Appendix A1, and the axisymmetric particle case has been experimentally validated using gold nanorods in an electric field [5,29]. For a particle

with fully random orientation, the averaged mobility is

$$\langle Z_p \rangle = \frac{1}{3}q \left( \frac{1}{K_1} + \frac{1}{K_2} + \frac{1}{K_3} \right). \quad (23)$$

### C. Approach III: Mobility of a nonspherical particle from the averaged-drag force

If Brownian rotation is fast compared to the translational relaxation time of a nonspherical particle, then Eq. (20) cannot be applied assuming the particle evolves from one orientation to another and thus the averaged-drift-velocity approach is invalid. Considering an extreme situation of rotation around a single axis for which a  $2\pi$  rotation is sufficiently fast that its drift velocity does not respond to the particle orientation change, the drift velocity can then be treated as independent of particle orientation and always along the direction of the external force  $\vec{k}$ . In this situation, we can think that the external force is balanced by an orientation averaged drag force with the form expressed in Eq. (19) along the external force direction,

$$F_{\text{external}} = -\langle \vec{F}_{\text{drag}} \rangle \cdot \vec{k} = \langle \hat{K} \cdot \vec{V}_d \rangle \cdot \vec{k} \quad (24)$$

and

$$\vec{V}_d = V_d \vec{k}. \quad (25)$$

The prerequisite of this approach suggests that it is valid for very small ions and for small particles in the free molecular regime, and is similar to the averaged-collision-integral approach by averaging the drag force orientationally and assuming the drift velocity independent of particle orientation. The difference between the two is that drag force in this approach is expressed in tensor form while in the averaged-collision-integral approach the drag force is expressed in a collision integral or cross-section area. In Sec. IV, we will show that for a cylindrical rod in the free molecular regime at random orientation, this approach is identical to the averaged-collision-integral approach with a short-range potential (hard collisions). The explicit expressions of the three principle components of friction coefficient tensor  $\hat{K}$  used in Eq. (24) for hard-body rods and prolate spheroids in free molecular regimes were provided in Li *et al.* [28]. A general expression of friction coefficient tensor for any hard-body convex particles in free molecular can be obtained in de la Mora [37] and Garcia-Ybarra and Rosner [38].

Combining Eqs. (24) and (25) and considering the external force is an electric force, we have

$$Z_p = V_d / E = q / \langle \vec{k} \cdot \hat{K} \cdot \vec{k} \rangle. \quad (26)$$

Expressing Eq. (26) in terms of the Euler angles  $\varphi, \psi, \theta$ , and considering particle orientation distribution function  $f(\varphi, \psi, \theta)$ , then Eq. (26) becomes

$$Z_p = q / (K_1 \langle \sin^2 \theta \sin^2 \psi \rangle + K_2 \langle \sin^2 \theta \cos^2 \psi \rangle + K_3 \langle \cos^2 \theta \rangle). \quad (27)$$

For random oriented particles, the averaged mobility is

$$Z_p = \frac{3q}{K_1 + K_2 + K_3}. \quad (28)$$

The expressions of the mobility for more orientational probability cases and the expressions of the averaged drag forces are shown in Appendix A2.

### III. MATERIALS AND EXPERIMENTAL METHODS<sup>1</sup>

In order to employ a nonspherical particle with a well-defined size and monodispersity, we chose a colloidal gold nanorod (Nanopartz Inc.; MUTAB coated conjugated gold nanorods; 10 nm, SPR = 2000 nm, 0.25 mg, 1 mL; C12N-10-2000-TMU-0.25) which has a dimensionality of 17 nm × 270 nm under TEM analysis. Aerosolized gold nanorods were generated by electrospray (model 3480, TSI Inc.) using a 40- $\mu$ m inner diameter capillary and operated with a carrier gas of 1.2 L/min of purified air. The aerosolized particles were then passed over a radioactive Po-210( $\alpha$ ) source to reduce the charge to a well-defined charge distribution with most neutral and singly charged particles [39]. The neutralized dry particles entered a differential mobility analyzer (model 3081 Long DMA column, TSI Inc.) for particle mobility measurement and were subsequently counted with an ultrafine CPC (model 3025A, TSI Inc.). By scanning the center rod voltage of the DMA, different mobility particles can be exacted to build a mobility distribution for a given particle population. The mobility can be converted to an equivalent spherical diameter, (i.e., mobility diameter) which will be discussed in Sec. IV. The DMA measurement was operated at room temperature and 1 atm pressure. More details on the measurement method can be found in Li *et al.* [6,40] and Guha *et al.* [41]. The long DMA was set with a sheath flow of 5 L/min and an aerosol flow of 0.7 L/min to guarantee the gold nanorods detected at a very low voltage ( $\sim$ 474 V). At this low voltage, the gold nanorods basically were randomly oriented. To avoid the effects of time varying electric field as the particles go through the DMA, we operated the DMA in the step mode, and kept the step sufficiently long to ensure a complete transit through the DMA system before the voltage was changed (45 s).

The mobility size of the gold nanorods was calibrated using 100.7-nm NIST standard reference material (polystyrene latex spherical particle) [5]. The measurements with the standard reference material (100.7 nm) and the gold nanorod were repeated three times respectively, and the assignment of DMA detection voltage was obtained by averaging the three means of the Gaussian fits to the experimental profile. The exact sheath flow value was assigned by measurement of the 100.7-nm NIST standard reference material at the same condition as the gold nanorod measurement. Using this calibrated sheath flow value, the mobility sizes of the gold rod could be determined.

### IV. RESULTS AND DISCUSSIONS

The averaged-collision-integral approach considers the molecular collision mechanism and obtains the averaged

mobility of nonspherical particles based on a collision integral calculation, while the averaged-drag-force approach calculates particle mobility by averaging the drag force in a tensor form, but both approaches are proposed for small ions and for small particles in the free molecular regime, and both have a common assumption, that the drift velocity is independent of particle orientation and always along the direction of external force if the Brownian rotation is fast compared with the particle translational relaxation process. We will show that for a cylinder rod in the free molecular regime at random orientation for short-range interactions (hard collisions), the averaged-drag-force approach is identical to the averaged-collision-integral approach. On the other hand, the averaged-drift-velocity approach assumes that the particle Brownian rotation is slow compared with the particle translational relaxation time, so that at each orientation the drag force is immediately balanced by the external force and the drift velocity of a nonspherical particle depends on particle orientation. So the averaged-drift-velocity approach is expected to apply to relative larger particles. Theoretically, the averaged-drift-velocity approach and the averaged-drag-force approach provide two limit mobility values. One way to assess if the Brownian motion of a cylindrical particle is “slow” or “fast” by comparing to the particle translational relaxation process was shown in Li (2012) [30] using the rotational diffusion coefficient expression in the free molecular regime [42] and in the continuum regime [43].

Mobility based on the averaged-collision integral can be calculated using the open source software program MOBICAL. Similarly, for a convex particle, using the general expression of friction coefficient tensor [37,38], theoretically, the mobility for any convex shape could also be obtained using averaged-drift-velocity or averaged-drag-force approaches for small ions and for small particles in the free molecular regime. Without losing generality, in this section, we discuss the three approaches by applying them to a rod with fully random orientation where we have analytical expressions. Then the three approaches will be compared with the experimental measurement of a gold nanorod (a good example of a straight rigid rod), and with the calculation results for GroEL (a protein) in the literature.

For the three approaches applied in this section with fully random orientation, the expressions of mobility diameters are summarized in Table II.

#### A. Application to a rod in fully random orientation for a short-range interaction (hard collision)

We now compare the calculation results from the three approaches applied to a rod in a fully random orientation.

The averaged projection area in Eq. (10) for any crystal structure of ion or particle can be obtained by the open source software program MOBICAL. For a particle with cylindrical geometric shape (diameter  $d_r$ , length  $L_r$ ) for hard collisions, the exact analytical expression is derived as

$$\langle Q_{pa} \rangle = \frac{\pi}{4} \left( d_r L_r + \frac{1}{2} d_r^2 \right) = \frac{\pi}{4} d_r^2 \left( \beta + \frac{1}{2} \right). \quad (29)$$

The averaged projection area diameter is defined as  $d_{pa} = \sqrt{4\langle Q_{pa} \rangle / \pi}$ , which has been proved equivalent to the mobility

<sup>1</sup>Mention of commercial equipment, instruments, or materials identified in this paper does not imply recommendation or endorsement by the University of Maryland or the National Institute of Standards and Technology.

diameter  $d_m$  of a convex particle for short-range interactions (hard collisions) in the free molecular regime in Sec. IIA.

The average mobility of a fully random rod can also be obtained by Eqs. (23) and (28) for averaged-drift-velocity and averaged-drag-force approaches, respectively. Each of the three principle components of the friction coefficient tensor ( $K_1$ ,  $K_2$ , and  $K_3$ ) used in the two approaches for a rod in the free molecular regime [28] are calculated based on Dahneke [44]. The averaged mobilities  $Z_p$  are then converted to an equivalent spherical diameter  $d_m$  as

$$Z_p = \frac{2\lambda(A_1 + A_2)q}{3\pi\eta d_m^2}, \quad (30)$$

where,  $A_1 = 1.165$ , and  $A_2 = 0.483$ , respectively for solid particles with averaged free path  $\lambda = 67.3$  nm for ambient air at sea level and 23 °C given by Kim *et al.* [35].  $d_m$  is denoted as  $d_{adv}$  from the averaged-drift-velocity approach and as  $d_{adf}$  from the averaged-drag-force approach.

**The averaged-drag-force approach for a nanorod in the free molecular regime at random orientation is identical to averaged-collision-integral approach with a short-range potential (hard collision).** The mobility of a rod at random orientation from the averaged-drag-force approach is given by Eq. (28) where the friction coefficient components  $K_1$ ,  $K_2$ , and  $K_3$  can be obtained from Dahneke's drag force expression of a rod (diameter  $d_r$ ; length  $L_r$ ; aspect ratio  $\beta = L_r/d_r$ ) in the free molecular regime as [Li *et al.* [28], Eqs. (A1) and (A2)]

$$K_1 = K_2 = \frac{1}{2\phi} \frac{\pi\eta d_r^2}{2\lambda} \left[ \left( \frac{\pi - 2}{4} \beta + \frac{1}{2} \right) f + 2\beta \right]$$

and

$$K_3 = \frac{1}{2\phi} \frac{\pi\eta d_r^2}{2\lambda} \left[ \left( \beta + \frac{\pi}{4} - 1 \right) f + 2 \right],$$

where  $\phi = 0.491$  used in Allen and Raabe [33], and  $\phi = 0.5$  used in Dahneke [44]. Thus, we have

$$Z_p = \frac{3q}{K_1 + K_2 + K_3} = \frac{6q\lambda\phi}{2\pi\eta d_r^2(1 + \pi f/8)(\beta + 1/2)}.$$

Considering the expression of coefficient of viscosity in Eq. (15), and the "enhancement factor" in Eq. (11), we obtain

$$Z_p = \frac{1}{\xi} \frac{3q}{16N} \sqrt{\frac{2\pi}{m_r k_B T}} \frac{1}{\pi d_r^2 (\beta + 1/2)/4},$$

which is exactly equivalent to the mobility of a rod obtained from the averaged-collision-integral approach in Eq. (13) considering the averaged projection area ( $Q_{pa}$ ) is given by Eq. (29) for a rod. The mobility diameter and drag force of a rod are also shown to be identical between the averaged-drag-force approach and the averaged-collision-integral approach for a short-range potential (hard collision).

$d_{pa}$ ,  $d_{adv}$ , and  $d_{adf}$  are calculated for rods with various diameters and aspect ratios in air, and shown in Table III. Table III shows that the equivalent diameters from the averaged-collision-integral approach (here an averaged-projected-area diameter) ( $d_{pa}$ ) and averaged-drag-force approach ( $d_{adf}$ ) are identical to each other, which is a valid test for Dahneke's expression of a rod in free molecular regime [44]. Based on Table III, the averaged-drift-velocity approach

TABLE III. The averaged projected diameter  $d_{pa}$ , and the mobility diameters from averaged-drift-velocity  $d_{adv}$ , and averaged-drag-force approaches  $d_{adf}$ , respectively, are shown for various diameters and aspect ratios of rods with random orientation.

Diameter $d_r$ (nm)	Aspect ratio $\beta$	$d_{pa} = d_{adf}$ (nm)	$d_{adv}$ (nm)
1	2	1.6	1.6
1	5	2.3	2.2
1	10	3.2	3.0
1	20	4.5	4.2
5	2	7.9	7.8
5	5	11.7	11.2
5	10	16.2	15.2
5	20	22.6	20.9
15	2	23.7	23.4
15	5	35.2	33.6
15	10	48.6	45.5

provides a smaller mobility diameter (or a larger mobility) than the other two approaches, which give identical results.

### B. Comparing the three approaches with the experimental result for a gold nanorod

The gold nanorod is a good example of a straight rigid rod (length  $L_r \approx 270$  nm and diameter  $d_r \approx 17$  nm from TEM). One length scale of this gold nanorod is smaller than the mean free path ( $\sim 67$  nm) and one is larger. As pointed out in one of our previous works [5], for those dimensions (17 nm  $\times$  270 nm), the free molecule transport properties resulted in better agreement with the measured electrical mobility than using transition theory transport properties. Also, based on literature, the long-range potential is expected to take some effect only for very small particles, less than 3 nm [45], so for the gold rod, the long-range potential can be neglected and hard-collision expressions are applied. Considering the finite diameter of the bath gas molecules,  $d_g = 0.3$  nm, which increases  $L_r$  and  $d_r$  by 0.3 nm [7], the calculated values are shown in Table IV. We note here that for any comparison between experiment and model, correction for the bath gas should only be performed for either the model or the experiment, and not both as has been done in some cases, where the effect was considered twice [19].

The experimental value of the mobility of gold nanorods at very low electric field (random orientation) was measured using the DMA and converted to a mobility diameter of  $66.8 \pm 0.1$  nm based on Eq. (30), which falls between the two limit values from the averaged-drift-velocity approach, 64.3 nm, and the averaged-drag-force approach of 69.5 nm. The results are consistent with the assessment in Li (2012, pp. 165–169) [30] to determine if Brownian motion of a cylindrical particle is "slow" or "fast," by scaling to the particle translational relaxation time. In Li (2012, pp. 165–169) [30], a characteristic time  $\tau_0$  was defined for Brownian rotation, and compared with the translational relaxation time  $\tau_{t,rod} = m/K_{random}$ , where  $m$  is the mass of the rod,  $1/K_{random} = 2/K_1 + 1/K_3$ , and  $K_1$ ,  $K_3$  were given in the previous section for a rod in the free molecular regime. Based on Li's estimation,

TABLE IV. The gold nanorod experimental mobility diameter from DMA is compared with the three diameters calculated from three approaches. The experimental value falls in between the two limit values from averaged-drift-velocity and averaged-drag-force approaches.

Diameter $d_r$ (nm)	Aspect ratio $\beta$	Experimental mobility diameter by DMA (nm)	$d_{pa} = d_{adf}$ (nm)	$d_{adv}$ (nm)
17.3	270.3/17.3	$66.8 \pm 0.6^a$	$69.5 \pm 2.7^b$	$64.3 \pm 2.5^b$

<sup>a</sup>The experimental mobility diameter of the gold nanorod reported in one of our previous works [5] was converted from measured mobility based on Cunningham's slip correction factor instead of its limit at the free molecular regime, i.e., Eq. (30), thus is different from the mobility diameter shown above. The combined uncertainty for mobility size is based on three repeat experiments, the 0.47% uncertainty in the 100.7-nm calibration standard, and the flow rate calibration using 100.7-nm standards.

<sup>b</sup>The uncertainty for mobility size is from the 4% uncertainty in the TEM measurement.

if  $\tau_0/\tau_{t,rod} < 1$ , then Brownian rotation is considered fast, and the averaged-drag-force approach applies. If  $\tau_0/\tau_{t,rod} > 482$ , Brownian rotation is considered slow, and the averaged-drift-velocity approach applies. Using the density of bulk gold, the translational relaxation time of the randomly oriented gold nanorod is calculated  $\sim 3.8 \times 10^{-7}$  s, and  $\tau_0/\tau_{t,rod}$  is  $\sim 50$ , and the mobility should fall between the two limits, which in fact it does based on the experimental results in Table IV.

### C. Comparing the three approaches for the GroEL protein

The geometric approximation for the protein GroEL 14-mer is a cylinder with a length  $L \sim 14$  nm, and as base diameter  $\sim 13$  nm [13,19]. Using atomic coordinates derived from x-ray diffraction data of GroEL 14-mer and using a modified version of software program MOBCAL [2,4], the averaged projection area has been calculated to be 220 nm<sup>2</sup> in one source [13], and 217.6 nm<sup>2</sup> in another [19]. To compare with the result from the software program, Hogan *et al.* [19] used a heptagonal cylinder to represent the protein and obtained a projected area of 197 nm<sup>2</sup> considering the finite diameter of air 0.3 nm [7].

Using the three approaches in this work and approximating GroEL as a rod with length = 14.3 nm and diameter = 13.3 nm accounting for the finite diameter of air 0.3 nm [7], we calculate the results for GroEL in Table V. The projected area ( $\Omega_{pa}$ ) is based on Eq. (29).  $A_{adv}$  and  $A_{adf}$  are equivalent areas converted from  $d_{adv}$  and  $d_{adf}$  by  $A = \pi d^2/4$ , respectively. All three values, 218.8, 218.8, and 218.8 nm<sup>2</sup>, from the three approaches in this work are very close to the reported projected areas, 217.6 and 220 nm<sup>2</sup> [13,19]. The quality of this result is probably better

than should be expected given the uncertainty in the equivalent cylinder dimensions of the molecule.

## V. CONCLUSIONS

We propose an approach to obtain the mobility of nonspherical particles by averaging the drag force orientationally, and summarize and extend two other approaches common in the literature for particles in the free molecular regime, averaged-collision-integral and averaged-drift-velocity. In the averaged-collision-integral approach, the inelastic interaction, which has been commonly ignored in most literature, was considered and the collision integral theory for a spherical particle in Li and Wang [8] was extended to a convex nonspherical particle. The focus of the analysis was on hard collision though the general expression for a long-range force is included. This extended collision integral was derived and simplified to an averaged projection area multiplied by an enhancement factor for hard collisions. This enhanced factor was well used in literature based on the theory of spherical particles. We have derived this enhancement factor based on kinetic theory by applying the approach of Shvartsburg and Jarrold [2] to diffuse reflections. We also showed that the averaged projection area of a convex particle for hard collisions is equal to its mobility diameter. The approach of Li *et al.* [28] for computing the average mobility for an axially symmetric particle by averaging its drift velocity has been further extended to a general form and for more symmetric cases. We also pointed out that this averaged-drift-velocity approach is only valid for relatively large particles where the Brownian rotation is slow compared with the particle translational relaxation time. For very small ions and particles where the Brownian rotation is fast compared

TABLE V. Using the three approaches in this work and approximating GroEL as a rod with length = 14.3 nm and diameter = 13.3 nm accounting for the finite diameter of air 0.3 nm, we calculated the results of GroEL in the table, and compared to the values from software program using the crystal structure of GroEL, and also compared with the value calculated from Hogan's model.

Diameter $d_r$ (nm)	Aspect ratio $\beta$	$\langle \Omega_{pa} \rangle$	$\langle \Omega_{pa} \rangle$	$\langle \Omega_{pa} \rangle$	$\langle \Omega_{pa} \rangle = A_{adf}$	$A_{adv}$
		Obtained from MOBCAL (nm <sup>2</sup> )	Obtained from MOBCAL (nm <sup>2</sup> )	Hogan's model (nm <sup>2</sup> )	this work (nm <sup>2</sup> )	this work (nm <sup>2</sup> )
13.3	14.3/13.3	217.6 <sup>a</sup>	220 <sup>b</sup>	197 <sup>a</sup>	218.8	218.8

<sup>a</sup>Hogan *et al.* [19].

<sup>b</sup>van Duijn *et al.* [13].

with the particle translational rotation we propose an averaged-drag-force approach which calculates particle mobility by averaging the drag force in a tensor form. The three approaches were then compared with each other by being applied to a randomly oriented rod. We show that for a cylinder in the free molecular regime at random orientation, the averaged-drag-force approach is identical to the averaged-collision-integral approach with short-range potentials. We also compared the calculation results of the three approaches to the experimental value of monodisperse gold nanorods, which are rigid rods, and showed that the experimental value falls between the two limit calculated values from the averaged-drift-velocity approach and the averaged-drag-force approach as expected. Finally, we showed that the calculation results for GroEL protein from the software programs in the literature are in good agreement with our calculations using the three approaches in this work.

#### APPENDIX A: EULER ANGLES $\Phi$ , $\Psi$ , $\Theta$ , AND THE DERIVATIONS IN AVERAGED-DRIFT-VELOCITY APPROACH AND AVERAGED-DRAG-FORCE APPROACH

A space fixed coordinate system  $(x, y, z)$  with unit vector  $(\vec{i}, \vec{j}, \vec{k})$  respectively, and a particle body fixed coordinate system  $(x', y', z')$  with unit vector  $(\vec{i}', \vec{j}', \vec{k}')$  are shown in Fig. 1, where  $z$  direction (unit vector  $\vec{k}$ ) is chosen along the external force direction. Three Euler angles  $\varphi$ ,  $\psi$ ,  $\theta$ , relate the body fixed coordinate system to the space fixed one [46].

Assuming that the friction coefficient is in a tensor form, the drag force is expressed as [22]

$$\vec{F}_{\text{drag}} = -\hat{K} \cdot \vec{V}_d, \quad (\text{A1})$$

where  $\hat{K}$  is the friction coefficient tensor and  $\vec{V}_d$  is the drift velocity of the particle.

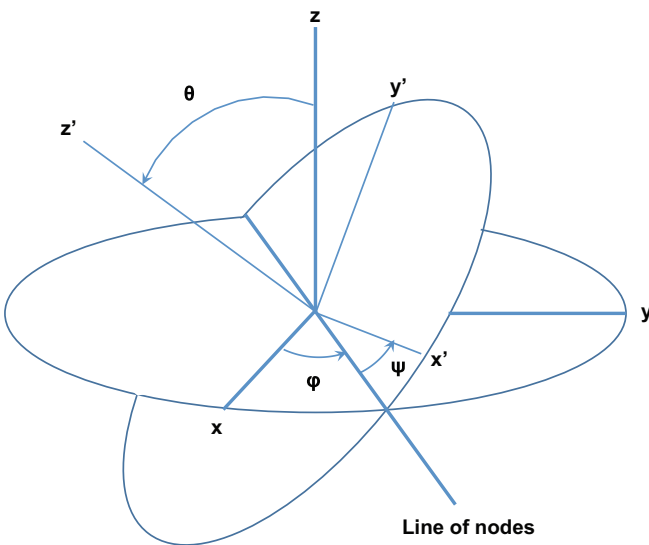


FIG. 1. (Color online) Three Euler angles  $\varphi$ ,  $\psi$ ,  $\theta$ , relate the particle body fixed coordinate system  $(x', y', z')$  to the space fixed coordinate system  $(x, y, z)$ .

#### 1. The velocity and mobility expressions in averaged-drift-velocity approach

Assuming at each orientation of the particle the drag force is balanced by the electric force, we obtain

$$\hat{K} \cdot \vec{V}_d = q\vec{E} \quad (\text{A2})$$

and

$$\vec{V}_d = q\hat{K}^{-1} \cdot \vec{E}. \quad (\text{A3})$$

If we define the particle body fixed coordinate system  $(\vec{i}', \vec{j}', \vec{k}')$  parallel to the three principal axes of the tensor  $\hat{K}$  of the particle, then

$$\vec{V}_d = V_{d,x}\vec{i} + V_{d,y}\vec{j} + V_{d,z}\vec{k},$$

$$V_{d,x} = qE(K_1^{-1}a_1 + K_2^{-1}a_2 + K_3^{-1}a_3),$$

$$V_{d,y} = qE(K_1^{-1}b_1 + K_2^{-1}b_2 + K_3^{-1}b_3),$$

$$V_{d,z} = qE(K_1^{-1}c_1 + K_2^{-1}c_2 + K_3^{-1}c_3),$$

$$a_1 = \cos\psi \cos\varphi \sin\theta \sin\psi - \cos\theta \sin\varphi \sin^2\psi \sin\theta,$$

$$a_2 = -\sin\psi \cos\varphi \sin\theta \cos\psi - \cos\theta \sin\varphi \cos^2\psi \sin\theta,$$

$$a_3 = \sin\theta \sin\varphi \cos\theta,$$

$$b_1 = \cos\psi \sin\varphi \sin\theta \sin\psi + \cos\theta \sin\varphi \sin^2\psi \sin\theta,$$

$$b_2 = -\sin\psi \sin\varphi \sin\theta \cos\psi + \cos\theta \cos\varphi \cos^2\psi \sin\theta,$$

$$b_3 = -\sin\theta \cos\varphi \cos\theta,$$

$$c_1 = \sin^2\theta \sin^2\psi, \quad c_2 = \sin^2\theta \cos^2\psi, \quad c_3 = \cos^2\theta,$$

where  $K_1$ ,  $K_2$ , and  $K_3$  are three principal components of the friction coefficient tensor.

If particle orientation follows a distribution function  $f(\varphi, \psi, \theta)$ , then

$$\langle \vec{V}_d \rangle_{\vec{k}} = \langle V_{d,z} \rangle$$

$$= qE(K_1^{-1}\langle \sin^2\theta \sin^2\psi \rangle + K_2^{-1}\langle \sin^2\theta \cos^2\psi \rangle + K_3^{-1}\langle \cos^2\theta \rangle). \quad (\text{A4})$$

In some specific situations, such as  $f(\varphi, \psi, \theta) = f(\psi, \theta)$ ,  $f(\varphi, \psi, \theta) = f(\theta)$ , or  $f(\varphi, \psi, \theta) = 1/8\pi^2$ ,  $\langle V_{d,x} \rangle$  and  $\langle V_{d,y} \rangle$  vanish, and we have  $\langle \vec{V}_d \rangle = \langle V_{d,z} \rangle \vec{k}$  or  $\langle \vec{V}_d \rangle = \langle V_d \rangle \vec{k}$ , i.e., the averaged drift velocity  $\langle \vec{V}_d \rangle$  only has one component along the external force direction ( $\vec{k}$  direction), and the averaged mobility can be conveniently obtained by  $\langle Z_p \rangle = \langle V_d \rangle / E$ . We discuss three such cases below.

(i) *Fully random* [22]. The averaged mobility is

$$\langle Z_p \rangle = \frac{1}{3}q \left( \frac{1}{K_1} + \frac{1}{K_2} + \frac{1}{K_3} \right). \quad (\text{A5})$$

(ii) *Axisymmetric particles with orientation distribution  $f(\theta)$*  [28]. For axially symmetric particles,  $K_1 = K_2 = K_{\perp}$  where  $K_{\perp}$  is the principal component of the friction coefficient tensor perpendicular to the axial direction and  $K_3 = K_{\parallel}$  where  $K_{\parallel}$  is the component parallel to the axial direction. If the orientation distribution can be expressed as  $f(\theta)$ , for example, the axisymmetric particles orientated based on Boltzmann

angular distribution due to Brownian rotation (Appendix B), we obtain

$$\langle Z_p \rangle = q[K_{\perp}^{-1} + (K_{\parallel}^{-1} - K_{\perp}^{-1})\langle \cos^2 \theta \rangle], \quad (\text{A6})$$

where  $\langle \cos^2 \theta \rangle = \int_0^{\pi} \cos^2 \theta f(\theta) \sin \theta d\theta$  is the orientationally averaged  $\cos^2(\theta)$  and  $\int_0^{\pi} f(\theta) \sin \theta d\theta = 1$ .

The calculation of Eq. (A6) was described in detail in Li *et al.* [28] and showed that the averaged mobility is a function of particle orientation which in turn depends on the magnitude of the electric field. Equation (A6) was experimentally verified using gold nanorods [5,29].

(iii) *More general symmetric case with orientation distribution*  $f(\psi, \theta)$ . One can extend the axisymmetric case above to a more symmetric case where the orientation distribution  $f(\psi, \theta)$  is only a function of  $\psi$  and  $\theta$ , for example a uniform right angled parallelepiped orientated based on Boltzmann angular distribution due to Brownian rotation (Appendix B). In this case the mobility becomes

$$\langle Z_p \rangle = q(K_1^{-1}\langle \sin^2 \theta \sin^2 \psi \rangle + K_2^{-1}\langle \sin^2 \theta \cos^2 \psi \rangle + K_3^{-1}\langle \cos^2 \theta \rangle). \quad (\text{A7})$$

Furthermore, if  $K_1 = K_2$ , such as a uniform right angled parallelepiped with square bases, Eq. (A7) becomes

$$\langle Z_p \rangle = q[K_1^{-1} + (K_3^{-1} - K_1^{-1})\langle \cos^2 \theta \rangle]. \quad (\text{A8})$$

We note that all the averaging above is related to orientation distribution  $f(\psi, \theta)$ . All the averages above are related to orientation distribution  $f(\psi, \theta)$  as

$$\begin{aligned} \langle X \rangle &= \int_0^{2\pi} d\varphi \int_0^{\pi} d\theta \sin \theta \int_0^{2\pi} d\psi f(\psi, \theta) X(\psi, \theta) \\ &= \frac{1}{2\pi} \int_0^{\pi} d\theta \sin \theta \int_0^{2\pi} d\psi f(\psi, \theta) X(\psi, \theta). \end{aligned} \quad (\text{A9})$$

If  $K_1 = K_2 = K_3$  such as a uniform cubic,

$$\langle Z_p \rangle = qK_1^{-1}. \quad (\text{A10})$$

## 2. The drag force expressions in averaged-drag-force approach

In the averaged-drag-force approach, we can think that the external force is balanced by an orientation averaged drag force with the form expressed in Eq. (A1) along the external force direction,

$$F_{\text{external}} = -\langle \vec{F}_{\text{drag}} \rangle \cdot \vec{k} = \langle \hat{K} \cdot \vec{V}_d \rangle \cdot \vec{k} \quad (\text{A11})$$

and

$$\vec{V}_d = V_d \vec{k}. \quad (\text{A12})$$

Combine Eqs. (A11) and (A12) and consider that the external force is an electric force; we have

$$qE = V_d \langle \vec{k} \cdot \hat{K} \cdot \vec{k} \rangle$$

and

$$Z_p = V_d/E = q/\langle \vec{k} \cdot \hat{K} \cdot \vec{k} \rangle. \quad (\text{A13})$$

If we define the particle body fixed coordinate system  $(\vec{i}', \vec{j}', \vec{k}')$  parallel to the three principal axes of the tensor  $\hat{K}$  of

the particle, then

$$\begin{aligned} \langle \hat{K} \cdot \vec{k} \rangle_i &= K_1 \langle a_1 \rangle + K_2 \langle a_2 \rangle + K_3 \langle a_3 \rangle, \\ \langle \hat{K} \cdot \vec{k} \rangle_j &= K_1 \langle b_1 \rangle + K_2 \langle b_2 \rangle + K_3 \langle b_3 \rangle, \\ \langle \hat{K} \cdot \vec{k} \rangle_k &= \langle \vec{k} \cdot \hat{K} \cdot \vec{k} \rangle = K_1 \langle c_1 \rangle + K_2 \langle c_2 \rangle + K_3 \langle c_3 \rangle, \end{aligned}$$

where  $K_1$ ,  $K_2$ , and  $K_3$  are three principal components. The expressions of  $a_1$  to  $c_3$  were shown in Appendix A1. If particle orientation follows a distribution function  $f(\varphi, \psi, \theta)$ , then Eq. (A13) becomes

$$Z_p = q/(K_1 \langle \sin^2 \theta \sin^2 \psi \rangle + K_2 \langle \sin^2 \theta \cos^2 \psi \rangle + K_3 \langle \cos^2 \theta \rangle). \quad (\text{A14})$$

All the averages in the above formula are related to orientation distribution  $f(\varphi, \psi, \theta)$  in the form of Eq. (8) in the main text.

Based on Eq. (A12), the averaged drag force can be expressed as

$$\langle \vec{F}_{\text{drag}} \rangle = -\langle \hat{K} \cdot \vec{V}_d \rangle = -\langle \hat{K} \cdot \vec{k} \rangle V_d.$$

In symmetric situations, such as  $f(\varphi, \psi, \theta) = f(\psi, \theta)$ ,  $f(\varphi, \psi, \theta) = f(\theta)$ , or  $f(\varphi, \psi, \theta) = 1/8\pi^2$ ,  $\langle \hat{K} \cdot \vec{k} \rangle_i$  and  $\langle \hat{K} \cdot \vec{k} \rangle_j$  vanish, and we have

$$\langle \vec{F}_{\text{drag}} \rangle = -\langle \vec{k} \cdot \hat{K} \cdot \vec{k} \rangle V_d \vec{k}. \quad (\text{A15})$$

Applying Eqs. (A15) and (A13) above to three symmetric situations, we have the following:

(i) *Fully random*,

$$\langle \vec{F}_{\text{drag}} \rangle = -\frac{K_1 + K_2 + K_3}{3} V_d \vec{k}, \quad (\text{A16})$$

$$Z_p = \frac{3q}{K_1 + K_2 + K_3}. \quad (\text{A17})$$

(ii) *Axisymmetric particles; orientation distribution*  $f(\theta)$ ,

$$\langle \vec{F}_{\text{drag}} \rangle = -[K_{\perp} + (K_{\parallel} - K_{\perp})\langle \cos^2 \theta \rangle] V_d \vec{k}, \quad (\text{A18})$$

$$Z_p = \frac{q}{K_{\perp} + (K_{\parallel} - K_{\perp})\langle \cos^2 \theta \rangle}, \quad (\text{A19})$$

where  $\langle \cos^2 \theta \rangle = \int_0^{\pi} \cos^2 \theta f(\theta) \sin \theta d\theta$  is the orientationally averaged  $\cos^2(\theta)$  and  $\int_0^{\pi} f(\theta) \sin \theta d\theta = 1$ .

(iii) *More general symmetric case with orientation distribution*  $f(\psi, \theta)$ . If orientation distribution function  $f(\psi, \theta)$  is only a function of  $\psi, \theta$ , for example, a uniform right angled parallelepiped, then

$$\begin{aligned} \langle \vec{F}_{\text{drag}} \rangle &= -(K_1 \langle \sin^2 \theta \sin^2 \psi \rangle + K_2 \langle \sin^2 \theta \cos^2 \psi \rangle \\ &\quad + K_3 \langle \cos^2 \theta \rangle) V_d \vec{k}, \end{aligned} \quad (\text{A20})$$

$$Z_p = \frac{q}{K_1 \langle \sin^2 \theta \sin^2 \psi \rangle + K_2 \langle \sin^2 \theta \cos^2 \psi \rangle + K_3 \langle \cos^2 \theta \rangle}. \quad (\text{A21})$$

If  $K_1 = K_2$ , such as a uniform right angled parallelepiped with square top and bottom,

$$\langle \vec{F}_{\text{drag}} \rangle = -[K_1 + (K_3 - K_1)\langle \cos^2 \theta \rangle] V_d \vec{k}, \quad (\text{A22})$$

$$Z_p = \frac{q}{K_1 + (K_3 - K_1)\langle \cos^2 \theta \rangle}. \quad (\text{A23})$$

All the averages above related to orientation distribution  $f(\psi, \theta)$  are defined as in Eq. (A9). If  $K_1 = K_2 = K_3$  such as a uniform cubic,  $\langle \vec{F}_{\text{drag}} \rangle = -K_1 V_d \vec{k}$ .

### APPENDIX B: ORIENTATION DISTRIBUTION DUE TO BROWNIAN ROTATION

If the particles are small enough, over the time scale of interest, the rotational Brownian motion will result in a steady state distribution of the orientation, i.e., Boltzmann angular distribution,

$$f(\varphi, \psi, \theta) = \frac{e^{-U/kT}}{\int_0^{2\pi} d\varphi \int_0^\pi d\theta \sin\theta \int_0^{2\pi} d\psi e^{-U/kT}},$$

where  $\int_0^{2\pi} d\varphi \int_0^\pi d\theta \sin\theta \int_0^{2\pi} d\psi f(\varphi, \psi, \theta) = 1$ , and  $U$  is the interaction energy between the particle and the external electric field and is addressed in detail in Li *et al.* [28].

(i) *Symmetric case with orientation distribution*  $f(\psi, \theta)$ . If the interaction energy  $U$  is only a function of  $\psi, \theta$ , then  $f(\varphi, \psi, \theta)$  becomes  $f(\psi, \theta)$ . Following we give an example by only considering the polarization energy  $U_p$ , that is,  $U = U_p$ . The interaction energy  $U$  is dominated by polarization energy  $U_p$  [5] and  $U_p$  is given by [47]

$$U_p = -\frac{1}{2} \vec{E} \cdot \hat{\alpha} \cdot \vec{E},$$

where  $\hat{\alpha}$  is the polarizability tensor. If we assume that  $U = U_p$ , then as long as the three principal axes of the friction coefficient tensor  $\hat{K}$  are the same as for polarizability tensor  $\hat{\alpha}$ , for example, a uniform right angled parallelepiped,  $f(\varphi, \psi, \theta)$  becomes  $f(\psi, \theta)$ ,

$$f(\psi, \theta) = \frac{e^{-U_p/kT}}{\frac{1}{2\pi} \int_0^\pi d\theta \sin\theta \int_0^{2\pi} d\psi e^{-U_p/kT}}, \quad (\text{B1})$$

where  $U_p = -\frac{E^2}{2}(\alpha_1 \sin^2 \theta \sin^2 \psi + \alpha_2 \sin^2 \theta \cos^2 \psi + \alpha_3 \cos^2 \theta)$  and  $(\alpha_1, \alpha_2, \alpha_3)$  are the principal components of the polarizability tensor.

(ii) *Axisymmetric particles with orientation distribution*  $f(\theta)$  [28]. The expression of Boltzmann angular distribution of  $f(\theta)$  for axisymmetric particles was described in detail in Li *et al.* [28].

### APPENDIX C: SIMPLIFYING THE AVERAGED COLLISION INTEGRAL IN EQ. (5) FOR A CONVEX PARTICLE WITH HARD COLLISIONS

If we extend Epstein's approach for a convex particle and simplify the collision calculation by still treating the particle surface as a smooth surface, then we need to compensate our calculation by incorporating a term of inelastic collisions (or diffuse reflections). And the orientationally averaged collision integral for a convex particle with rough surface is

$$\langle \Omega \rangle = f \langle \Omega_d \rangle + (1 - f) \langle \Omega_s \rangle, \quad (\text{C1})$$

where  $\Omega_s$  and  $\Omega_d$  are derived based on Li and Wang [8] as

$$\begin{aligned} \Omega_s(\varphi, \psi, \theta) &= \left( \frac{m_r}{2k_B T} \right)^3 \int_0^\infty dg \exp\left(-\frac{g^2}{2k_B T/m_r}\right) g^5 \\ &\times \int_0^{b_{\max}} db \{2\pi b [1 - \cos \chi(\varphi, \psi, \theta, g, b)]\}, \end{aligned} \quad (\text{C2})$$

$$\begin{aligned} \Omega_d(\varphi, \psi, \theta) &= \left( \frac{m_r}{2k_B T} \right)^3 \int_0^\infty dg \exp\left(-\frac{g^2}{2k_B T/m_r}\right) g^5 \\ &\times \int_0^{b_{\max}} db \left\{ 2\pi b \left[ 1 + \frac{1}{g} \sqrt{\frac{\pi k_B T}{2m_r}} \sin \frac{\chi(\varphi, \psi, \theta, g, b)}{2} \right] \right\}. \end{aligned} \quad (\text{C3})$$

$\chi(\varphi, \psi, \theta, g, b)$  is the scattering angle given by Li and Wang [2003, Eq. (16)] [8] [the long-range potential is included in the expression of  $\chi(\varphi, \psi, \theta, g, b)$ ],  $g$  is the relative velocity,  $b$  is the impact parameter,  $b_{\max}$  is the maximum extent of the particles in the radial direction. With the orientationally averaged collision integral  $\langle \Omega \rangle$  for a nonspherical convex particle in Eq. (C1), the drag force and the mobility are given by Eqs. (1) and (3) in the main text respectively.

If we only consider hard collisions and ignore long-range potential, the specular collision integral Eq. (C2) is equivalent to cross section  $Q_s$  [8,32],

$$\Omega_s = Q_s = 2\pi \int_0^{b_{\max}} b [1 - \cos \chi] db, \quad (\text{C4})$$

and the diffuse collision integral [Eq. (C3)] is equivalent to cross section  $Q_d$

$$\Omega_d = Q_d = 2\pi \int_0^{b_{\max}} b \left[ 1 + \frac{3\pi}{16} \sin \frac{\chi}{2} \right] db. \quad (\text{C5})$$

We note here that in the extended Epstein's approach, that is, Eq. (C1), both  $\langle \Omega_s \rangle$  and  $\langle \Omega_d \rangle$  should be calculated assuming the particle surface is smooth. Using the idea in Shvartsburg and Jarrold [2], we will show below that under this condition the two averaged collision integrals  $\langle \Omega_s \rangle$  and  $\langle \Omega_d \rangle$  can be

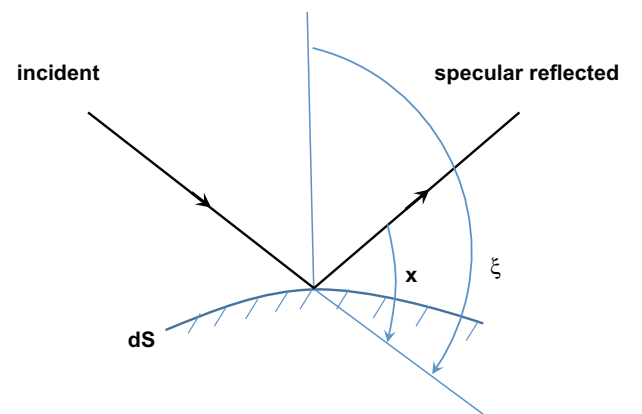


FIG. 2. (Color online) Demonstrating an incident molecule hitting small area  $dS$  on a convex particle and showing the relationship between angle  $\chi$  and angle  $\zeta$ .

further simplified to the averaged projected area multiplied by a factor.

Considering an infinitesimally small surface of a convex particle with area  $dS$  and the angle between the normal direction of this surface and the molecule incident direction is  $\zeta$  as shown in Fig. 2, the relationship between  $\zeta$  and  $\chi$  is

$$\zeta = \frac{\chi + \pi}{2}$$

and the projected area is

$$a_{\text{pa}} = -dS \cos \zeta.$$

Based on Eq. (C4), the specular collision integral element for this small surface is

$$\begin{aligned} \omega_S &= (1 - \cos \chi)a_{\text{pa}} = (1 - \cos \chi)(-\cos \zeta)dS \\ &= -2 \cos^3 \zeta dS. \end{aligned}$$

Averaging  $a_{\text{pa}}$  and  $\omega_S$  over all possible values of  $\zeta$  from  $\pi/2$  to  $\pi$ , we obtain

$$\langle a_{\text{pa}} \rangle = \frac{2\pi \int_{\pi/2}^{\pi} a_{\text{pa}} \sin \zeta d\zeta}{2\pi \int_{\pi/2}^{\pi} \sin \zeta d\zeta} = \frac{dS}{2} \quad (\text{C6})$$

and

$$\langle \omega_S \rangle = \frac{2\pi \int_{\pi/2}^{\pi} \omega_S \sin \zeta d\zeta}{2\pi \int_{\pi/2}^{\pi} \sin \zeta d\zeta} = \frac{dS}{2}. \quad (\text{C7})$$

Based on Eqs. (C6) and (C7), we have  $\langle a_{\text{pa}} \rangle = \langle \omega_S \rangle$ . Since any finite geometric surface can be considered as a set of infinitesimally small surfaces above, then the total averaged specular collision integral  $\langle \Omega_S \rangle$  is the sum of  $\langle \omega_S \rangle$ , as long as there is no mutual shadowing of small surfaces and no multiple collisions where molecules are reflected from one

small surface to another, which are satisfied by a convex and smooth surface. The total averaged projection area  $\langle \Omega_{\text{pa}} \rangle$  is the sum of  $\langle a_{\text{pa}} \rangle$ . So one concludes for any convex particle with a smooth surface

$$\langle \Omega_S \rangle = \langle \Omega_{\text{pa}} \rangle \quad (\text{C8})$$

Similarly, the diffuse collision integral element of Eq. (C3) for the infinitesimally small surface above is

$$\begin{aligned} \omega_d &= \left(1 + \frac{3\pi}{16} \sin \frac{\chi}{2}\right) a_{\text{pa}} \\ &= \left(1 + \frac{3\pi}{16} \sin \frac{\chi}{2}\right) (-\cos \zeta) dS \\ &= \left(1 - \frac{3\pi}{16} \cos \zeta\right) \cos \zeta dS. \end{aligned}$$

Averaging  $\omega_d$  over all possible values of  $\zeta$  from  $\pi/2$  to  $\pi$ , we obtain

$$\begin{aligned} \langle \omega_d \rangle &= \frac{2\pi \int_{\pi/2}^{\pi} \omega_d \sin \zeta d\zeta}{2\pi \int_{\pi/2}^{\pi} \sin \zeta d\zeta} = \left(\frac{\pi}{8} + 1\right) \frac{dS}{2} \\ &= \left(\frac{\pi}{8} + 1\right) \langle a_{\text{pa}} \rangle, \end{aligned}$$

which results in, for any convex particle with a smooth surface,

$$\langle \Omega_d \rangle = \left(\frac{\pi}{8} + 1\right) \langle \Omega_{\text{pa}} \rangle. \quad (\text{C9})$$

Combining Eqs. (C1), (C8), and (C9), we obtain the averaged collision integral for a convex particle with hard collisions as

$$\langle \Omega \rangle = \left(1 + \frac{\pi f}{8}\right) \langle \Omega_{\text{pa}} \rangle. \quad (\text{C10})$$

- 
- [1] G. Vonhelden, M. T. Hsu, N. Gotts, and M. T. Bowers, *J. Phys. Chem.* **97**, 8182 (1993).
- [2] A. A. Shvartsburg and M. F. Jarrold, *Chem. Phys. Lett.* **261**, 86 (1996).
- [3] A. A. Shvartsburg, S. V. Mashkevich, E. S. Baker, and R. D. Smith, *J. Phys. Chem. A* **111**, 2002 (2007).
- [4] B. T. Ruotolo, J. L. P. Benesch, A. M. Sandercock, S. J. Hyung, and C. V. Robinson, *Nat. Protoc.* **3**, 1139 (2008).
- [5] M. Li, R. You, G. W. Mulholland, and M. R. Zachariah, *Aerosol. Sci. Technol.* **47**, 1101 (2013).
- [6] M. Li, S. Guha, R. Zangmeister, M. J. Tarlov, and M. R. Zachariah, *Aerosol. Sci. Technol.* **45**, 849 (2011).
- [7] B. K. Ku and J. F. de la Mora, *Aerosol. Sci. Technol.* **43**, 241 (2009).
- [8] Z. Li and H. Wang, *Phys. Rev. E* **68**, 061206 (2003).
- [9] J. H. Ferziger and H. G. Kaper, *Mathematical Theory of Transport Processes in Gases* (North-Holland, Amsterdam, 1972).
- [10] W. C. Hinds, *Aerosol Technology: Properties, Behavior, and Measurement of Airborne Particles*, 2nd ed. (Wiley, New York, Chichester, 1999).
- [11] E. A. Mason and E. W. McDaniel, *Transport Properties of Ions in Gases* (Wiley, New York, 1988).
- [12] E. R. Brocker, S. E. Anderson, B. H. Northrop, P. J. Stang, and M. T. Bowers, *J. Am. Chem. Soc.* **132**, 13486 (2010).
- [13] E. van Duijn, A. Barendregt, S. Synowsky, C. Versluis, and A. J. R. Heck, *J. Am. Chem. Soc.* **131**, 1452 (2009).
- [14] P. S. Epstein, *Phys. Rev.* **23**, 710 (1924).
- [15] H. Tammet, *J. Aerosol Sci.* **26**, 459 (1995).
- [16] T. Wytttenbach, C. Bleiholder, and M. T. Bowers, *Anal. Chem.* **85**, 2191 (2013).
- [17] C. Bleiholder, T. Wytttenbach, and M. T. Bowers, *Int. J. Mass Spectrom.* **308**, 1 (2011).
- [18] C. J. Hogan and J. F. de la Mora, *J. Am. Soc. Mass Spectrom.* **22**, 158 (2011).
- [19] C. J. Hogan, B. T. Ruotolo, C. V. Robinson, and J. F. de la Mora, *J. Phys. Chem. B* **115**, 3614 (2011).
- [20] C. Larriba and C. J. Hogan, *J. Comput. Phys.* **251**, 344 (2013).
- [21] C. Larriba and C. J. Hogan, *J. Phys. Chem. A* **117**, 3887 (2013).
- [22] J. Happel and H. Brenner, *Low Reynolds Number Hydrodynamics, with Special Applications to Particulate Media* (Prentice-Hall, Englewood Cliffs, NJ, 1965).

- [23] B. E. Dahneke, *J. Aerosol Sci.* **4**, 139 (1973).
- [24] B. Dahneke, *Aerosol Sci. Technol.* **1**, 179 (1982).
- [25] Y. S. Cheng, M. D. Allen, D. P. Gallegos, H. C. Yeh, and K. Peterson, *Aerosol Sci. Technol.* **8**, 199 (1988).
- [26] Y. S. Cheng, *Chem. Eng. Commun.* **108**, 201 (1991).
- [27] D. W. Mackowski, *J. Aerosol Sci.* **37**, 242 (2006).
- [28] M. Li, G. W. Mulholland, and M. R. Zachariah, *Aerosol Sci. Technol.* **46**, 1035 (2012).
- [29] M. Li, R. You, G. W. Mulholland, and M. R. Zachariah, *Aerosol Sci. Technol.* **48**, 22 (2014).
- [30] M. Li, Dissertation, University of Maryland, College Park, 2012, available online at: <http://hdl.handle.net/1903/13627>
- [31] M. F. Mesleh, J. M. Hunter, A. A. Shvartsburg, G. C. Schatz, and M. F. Jarrold, *J. Phys. Chem.* **100**, 16082 (1996).
- [32] J. O. Hirschfelder, *Molecular Theory of Gases and Liquids* (Wiley, New York, 1954).
- [33] M. D. Allen and O. G. Raabe, *J. Aerosol Sci.* **13**, 537 (1982).
- [34] M. D. Allen and O. G. Raabe, *Aerosol Sci. Technol.* **4**, 269 (1985).
- [35] J. H. Kim, G. W. Mulholland, S. R. Kukuck, and D. Y. H. Pui, *J. Res. Natl. Inst. Stand.* **110**, 31 (2005).
- [36] L. F. Pease, D. H. Tsai, J. L. Hertz, R. A. Zangmeister, M. R. Zachariah, and M. J. Tarlov, *Langmuir* **26**, 11384 (2010).
- [37] J. F. de la Mora, *J. Aerosol Sci.* **33**, 477 (2002).
- [38] P. Garciaybarra and D. E. Rosner, *AIChE J.* **35**, 139 (1989).
- [39] A. Wiedensohler, *J. Aerosol Sci.* **19**, 387 (1988).
- [40] M. Li, S. Guha, R. Zangmeister, M. J. Tarlov, and M. R. Zachariah, *Langmuir* **27**, 14732 (2011).
- [41] S. Guha, M. Li, M. J. Tarlov, and M. R. Zachariah, *Trends Biotechnol.* **30**, 291 (2012).
- [42] M. Li, G. W. Mulholland, and M. R. Zachariah, *Aerosol Sci. Technol.* **48**, 139 (2014).
- [43] A. Ortega and J. G. de la Torre, *J. Chem. Phys.* **119**, 9914 (2003).
- [44] B. E. Dahneke, *J. Aerosol Sci.* **4**, 147 (1973).
- [45] Z. Li and H. Wang, *Phys. Rev. E* **68**, 061207 (2003).
- [46] H. Goldstein, C. P. Poole, and J. L. Safko, *Classical Mechanics*, 3rd ed. (Addison-Wesley, San Francisco, 2002).
- [47] C. J. F. Böttcher and O. C. v. Belle, *Dielectrics in Static Fields*, 2nd ed. (Elsevier Scientific, Amsterdam, New York, 1973).